Available online at www.sciencedirect.com
ScienceDirect
Physica B 385–386 (2006) 481–486
PHYSICA B
www.elsevier.com/locate/physb

Hydration of cement: The application of quasielastic and inelastic neutron scattering

Vanessa K. Peterson[a,b,*], Dan A. Neumann[b], R.A. Livingston[c]

[a]NIST Center for Neutron Research, National Institute of Standards and Technbology, Gaithersburg, MD 20899-8562, USA
[b]Department of Materials Science and Engineering, University of Maryland, College Park, MD 20742-2115, USA
[c]Federal Highway Administration McLean, VA 22101, USA

Abstract

Quasielastic and inelastic neutron scattering have been highlighted as excellent tools for studying the hydration of cement components. Here, the complimentary application of inelastic and time-resolved quasielastic neutron scattering to investigate the reaction kinetics during the crucial first 24 h of hydration will be highlighted. Some recent results include the interaction of tricalcium and dicalcium silicate during their combined hydration and the effect of the tricalcium silicate crystal form on hydration. The application of these tools for the prediction of strength development in hydrating mixtures is also presented.

PACS: 78.70.Nx; 81.05.Mh; 82.20.Bc

Keywords: Cement; Tricalcium silicate; Quasielastic neutron scattering; Inelastic neutron scattering

1. Introduction

Portland cement is an important construction material, with annual production currently exceeding 800 million metric tones. The structure, molecular composition, and physical properties of cement vary immensely during hydration. The complex details of this metamorphosis depend on both the structure and composition of the starting cement and the hydration conditions. Correlating the original composition and hydration kinetics with the final properties is the aim of this research. With this enhanced understanding, we will improve the ability to design and control the properties of the final product. Neutrons are well suited for the investigation of the structure and reaction mechanisms of cement, as they are particularly sensitive to hydrogen (and thus water), and are highly penetrating, allowing relatively large volumes to be sampled. This research reveals important details of the hydration of cement, and suggests ways to exploit them to improve cement performance.

Portland cement consists of many components. Tricalcium silicate (Ca_3SiO_5—C_3S) is the most important and abundant, comprising 50–70 wt% of the total. It reacts quickly with water and is the most important component for strength development, particularly in the first 28 d [1]. The hydration of C_3S is typically written as

$$2Ca_3SiO_5 + 7H_2O \rightarrow 3CaO \cdot 2SiO_2 \cdot 4H_2O + 3Ca(OH)_2 + 173.6\,kJ. \quad (1)$$

Dicalcium silicate (Ca_2SiO_4—C_2S) is the second most abundant component, comprising 15–30 wt% of clinker. C_2S reacts with water significantly more slowly than C_3S, contributing little to the strength development in cement at ages less than 28 d. It does, however, contribute substantially to the strength development beyond that time. The hydration of C_2S is

$$2Ca_2SiO_4 + 5H_2O \rightarrow 3CaO \cdot 2SiO_2 \cdot 4H_2O + Ca(OH)_2 + 58.6\,kJ \quad (2)$$

*Corresponding author. NIST Center for Neutron Research, National Institute of Standards and Technbology, Gaithersburg, MD 20899-8562, USA. Tel.: +1 301 975 8377; fax: +1 301 921 9847.
E-mail address: v.peterson@chem.usyd.edu.au (V.K. Peterson).

0921-4526/$ - see front matter © 2006 Published by Elsevier B.V.
doi:10.1016/j.physb.2006.05.253

It has been shown that in a cement paste at 28 d, about 70% of the total C_3S, and about 30% of the total C_2S, have reacted [1]. Compressive strength development is believed to run parallel to the course of the chemical reactions for the hydration of these two phases. Industrially, ordinary portland cement clinkers typically contain a C_3S to C_2S ratio of 3 to 1 [1].

The hydration of C_3S is often used as a model system to study the early stages of the setting process. The hydration of C_3S can be divided into three sections: initial hydrolysis followed by an induction period, nucleation and growth, and diffusion-limited hydration. Initial hydrolysis is the irreversible dissolution of the outer C_3S grain:

$$Ca_3SiO_5(s) + 3H_2O(l) \rightarrow 3Ca^{2+}(aq) + 4OH^-(aq) + H_2SiO_4^{2-}(aq). \quad (3)$$

This initial hydrolysis period when the C_3S grains rapidly release calcium and hydroxide ions, and a large amount of heat, is short; quickly slowing. The nucleation and growth period begins with the formation of calcium silicate hydrate (CSH) and $Ca(OH)_2$.

$$H_2SiO_4^{2-}(aq) + xCa^{2+}(aq) + (2x-2)OH^-(aq) + (y-x)H_2O(l) \leftrightharpoons (CaO)_x(SiO_2)\cdot(H_2O)_y, \quad (4)$$

$$Ca^{2+}(aq) + 2OH^-(aq) \leftrightharpoons Ca(OH)_2(s). \quad (5)$$

As the CSH layer thickens around the unreacted C_3S grains, it becomes increasingly difficult for water molecules to reach the C_3S. The speed of the reaction is now controlled by the rate at which water molecules diffuse through the CSH, known as diffusion-limited hydration. This coating thickens over time, causing the production of CSH to slow. The hydration will continue as long as water and C_3S are present.

As a result of the high sensitivity of neutrons for hydrogen, quasielastic neutron scattering (QENS) and inelastic neutron scattering (INS) can be applied to investigate both the hydration process and local structure of the hydration products that form as a result of these processes. QENS has recently been coupled with hydration models to enable the extraction of a thorough description of the hydration processes occurring in hydrating C_3S [2–13]. This method is reliable, can be performed in-situ, and allows density evaluation of the type of products formed.

The essential step in the hydration of cement components is the transfer of protons from free water to the solution ions, and then to the various end products of the reactions. Thus, one can follow the hydration reaction by determining the state of hydrogen as the reaction progresses. QENS provides a measure of the conversion of free water to structurally/chemically bound water and to water constrained in the pores of the cement paste. In this way, the mechanics of hydration can be probed using the QENS spectra, $S(Q, \omega)$, which is dominated by the incoherent scattering from hydrogen, as a function of the momentum transfer vector Q and energy change ω.

While QENS allows quantification of the *combined* hydration products, the method does not allow identification of specific quantities of either $Ca(OH)_2$ or CSH hydration products. The formation of multiple products in hydrating cement further complicates its analysis. INS can be applied complimentary to QENS to allow a separate determination of the hydration products, specifically the amount of $Ca(OH)_2$ present at any time during hydration of C_3S [4,5,14,15]. Together, these two techniques allow a more complete characterization of the crucial first portion of hydration, allowing the induction, nucleation and growth, and diffusion-limited hydration periods to be examined.

2. Experimental procedure

2.1. Sample preparation

Triclinic and monoclinic C_3S, as well as monoclinic C_2S powders were obtained from Construction Technology Laboratories (CTL, Skokie, IL[1]). Particle size analysis was conducted by CTL. Hydration took place using a water to cement mass ratio of 0.4, at the continuously monitored temperature of 30 °C. For QENS experiments, hydration took place inside a sealed Teflon bag inside a rectangular aluminum cell, and for INS experiments samples were sealed in the same Teflon bags and rolled inside an annular aluminum cell.

2.2. QENS measurement

QENS measurements were carried out using the Fermi chopper time-of-flight neutron spectrometer (FCS) [16] at the NIST Center for Neutron Research. The incident neutron wavelength used was 4.8 Å and the sample-to-detector distance was 2.29 m. The calculated elastic scattering energy resolution, ΔE, was 0.146 MeV. At low values of Q, the width of the quasielastic scattering from the total free water increases quadratically with Q as expected for Fickian diffusion. At higher Q, the width tends to level off to a more constant value. In view of this and the need to obtain adequate statistics, data were summed over the Q range of 2.0 to 2.3 $Å^{-1}$. This produced sufficient statistics, while minimizing the spread in the peak width due to the wide Q range.

The sample thicknesses were approximately 1 mm in the hydration cell, which was placed at a 45° angle to the incident neutron beam, in reflection geometry. QENS measurements were commenced 30 min after initial mixing,

[1]Manufacturers are identified in order to provide complete identification of experimental conditions, and such identification is not intended as a recommendation by the University of Maryland, NIST, or the Federal Highway Administration.

and the results were time averaged in 33 min slices. Data were collected continuously up to 55 h.

The profile utility PAN within the data analysis and visualization environment (DAVE) [17] was used for the analyses of QENS data. The QENS spectra were modeled using 3 components:

1. an elastic peak representing completely bound hydrogen using a resolution-limited Gaussian lineshape of width W_C and integrated area C, the evolution of C with time has been showed to follow heat evolution for the same hydration [11],
2. the narrowest quasielastic-broadened component arising from pseudo-bound hydrogen using a Lorentzian lineshape of width W_P and integrated area P, the evolution of P with time has been shown to track the development of surface area measured using small angle neutron scattering (SANS) [11],
3. a wider quasielastic-broadened component arising from hydrogen in the "free" water was modeled using 2 Lorentzian lineshapes of width W_{F_1} and W_{F_2}.

In all fits, the peak centers were constrained to be the same for each component. W_C was fixed to the width of the resolution function, shown to be a Gaussian function [12]. W_{F_1} and W_{F_2} were determined from data for the first seven time-averaged slices (3.85 h), where all the water was assumed to be in the free state. These values were fixed for all subsequent fits. For this determination, a Gaussian peak was included to account for contributions to the elastic line arising from the sample and hydration cell. In a similar manner, W_P was determined from the final seven time-averaged slices, and fixed for fits at previous reaction times. All three components were included in these fits. Thus, the number of free parameters included in the fits at each time was reduced to five: the peak centre, and the four integrated areas C, P, F_1 and F_2. Fig. 1 shows typical

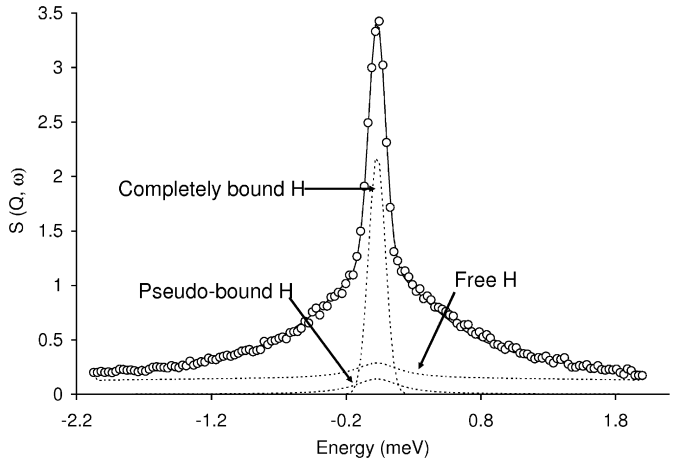

Fig. 1. Typical fitting of the QENS data at 5 h hydration time using DAVE, detailing the Gaussian and Lorentzian profiles as dotted lines. The overall fit is indicated by the solid line through the data (○).

Table 1
Typical peak fitting parameters derived from PAN fitting to QENS data during the hydration of C_3S.

Derived integrated area	Full-width at half-max. (MeV)
C (bound H)	$W_C = 0.146$ (fixed)
P (pseudo-bound H)	$W_P = 0.4$ (1)
F_1 (Free H)	$W_{F_1} = 1.22$ (3)
F_2 (Free H)	$W_{F_2} = 10.5$ (2)

Errors are absolute.

fitting of QENS data using DAVE, and Table 1 lists typical parameter values.

The fits of the individual, time-sliced spectra allowed a time-dependent bound-water index (BWI) to be constructed [10]:

$$\mathrm{BWI} = \frac{C+P}{C+P+(F_1+F_2)}. \quad (6)$$

The nucleation, growth, and diffusion limited hydration regimes of the BWI were then fit using the kinetic models that have previously been applied to C_3S hydration [2–7].

$$\mathrm{BWI}(t) = \mathrm{BWI}(0) + A[1-\exp\{-[k(t-t_i)]^n\}](t_i t t_d), \quad (7)$$

$$BWI(t) = BWI(0) + [1-\{[1-BWI(t_d)]^{1/3} - (R^{-1})(2D_i)^{1/2}(t-t_d)^{1/2}\}^3](t>t_d). \quad (8)$$

Here BWI(0) is the BWI at the end of the induction period, at the time t_i, and BWI(t_d) is the BWI at the time diffusion-limited kinetics begins, t_d, and R^{-1} is the mean inverse radius of the initial unhydrated particle size, determined from particle size distribution reports sent from CTL. For the mixtures, the R^{-1} corresponding to the dominant phase of the mixture was used. D_i is an effective diffusion coefficient, k the nucleation and growth reaction rate constant, and A the BWI had the nucleation and growth kinetics continued to infinite time. The exponent n has been determined experimentally to be 2.65 at 30 °C for C_3S, and this value was used to model QENS data for all mixtures [18]. t_i was established from the QENS hydration plots of t versus BWI(t). t_d was also established from these curves, from the narrow range that resulted in the smooth transition from nucleation and growth to diffusion-limited kinetics in the model. The free parameters in the model were D_i, A, and k, which were fitted to the data in the hydration curves. Fig. 2 shows a typical QENS BWI plot and hydration modeling.

2.3. INS measurement

INS data were obtained using the filter analyzer neutron spectrometer (FANS) on BT-4 [19] at the NIST Center for Neutron Research. The sample was oriented, in reflection, at a 45° scattering angle. A Cu (2 2 0) monochromator was used, with pre- and post-collimation of 60′ and 40′, respectively. Samples prepared identically to those used

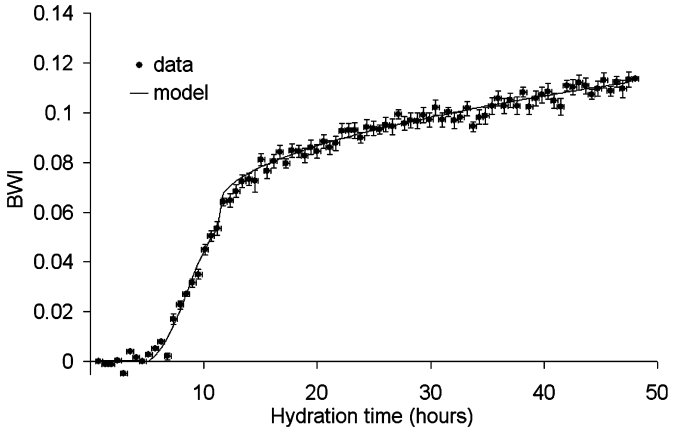

Fig. 2. Typical fitting of the diffusion models to the BWI derived from the QENS data for C_3S. Error bars represent absolute error.

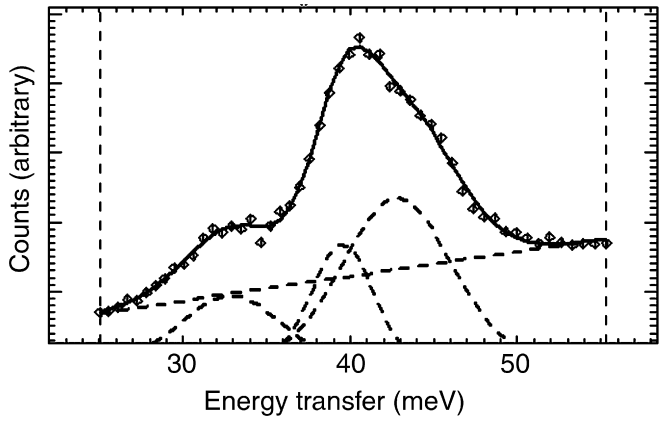

Fig. 3. Inelastic spectra for $Ca(OH)_2$ reference showing the three Gaussian and linear background components used in the fitting. The dotted lines represent the individual components, whilst the solid line represents the overall fit.

in the QENS experiment were analyzed, and reflection geometry data only were used. Data were collected over the energy range 25–55 MeV, the range covering the expected peak arising from $Ca(OH)_2$. The reference spectra were measured for a known mass of pure $Ca(OH)_2$ powder placed in an identical experimental set up as the hydrating samples. The sample and reference spectra were obtained under nominally identical conditions to ensure precision in the $Ca(OH)_2$ absolute mass calibration. Measurement of the integrated intensity of the 41 MeV peak enabled the absolute quantity of $Ca(OH)_2$ formed in the hydrated C_3S samples to be calculated. Background data consisting of an empty hydration cell were also collected.

The INS spectrum for each sample is representative of the density of states of the sample. DAVE was used for the data reduction and analyses of the INS data. The spectrum for the $Ca(OH)_2$ standard was modeled using 3 Gaussian lineshapes, and a linear background, detailed in Fig. 3.

The spectra for the hydrated C_3S were modeled using a single Gaussian lineshape and a linear background, due to poorer statistics.

3. Results and discussion

3.1. Interactions of components during hydration

Although it is widely recognized that the hydration of cement involves the *interaction* of the different components, very little is known about combined reactions. In particular, the less reactive and second most abundant component of cement, was not expected to significantly contribute to the overall hydration in the critical first 24 h. We have undertaken a systematic study of the hydration of controlled mixtures, by wt%, of C_3S and C_2S. The variation of kinetic parameters of the hydration obtained from the QENS data with composition are shown in Fig. 4. The peak in the parameters makes it apparent that at intermediate compositions the reaction cannot be simply described as a linear combination of the end points as would be the case if the two reactions had proceeded independently.

The parameter A, which represents the expected BWI after infinite time if the nucleation and growth mechanics had not been interrupted, is useful for predicting early strength development, as the amount of product (as well as type) correlates with cement strength. Parameter A exhibits a maximum for starting mixtures having a mass fraction of 80–95% C_3S. The concentration dependence of the effective diffusion constant of water, D_i, which limits the reaction rate in the diffusion-limited regime, correlates well with that observed for the parameter A. D_i has previously been shown to correlate with the permeability and perhaps the connectivity of the CSH [10]. Finally, the compressive strength (inset in Fig. 4) of mortars based on these mixtures measured after 28 d of hydration also correlates with the QENS results.

In order to quantify the amount of $Ca(OH)_2$ produced during the reaction, INS measurements were performed. The results, displayed in Fig. 5, reveal a clear maximum in the amount of $Ca(OH)_2$ produced at a mass fraction of about 90% C_3S.

Taken together, these neutron results demonstrate that the amount of product formed during early hydration times peak for compositions 85–90% C_3S. This is particularly surprising for $Ca(OH)_2$ since there is less total Ca in mixtures containing C_2S than in C_3S alone. Significant changes in D_i also suggest that the interaction affects the microstructure, and therefore the strength, of the product. Once again, the strengths of mortars of these mixtures cured for 28 d display a peak at 85% C_3S.

Hence, QENS and INS shows that a small amount of C_2S accelerates the hydration, even though C_2S is less reactive than C_3S. We attribute this effect to the presence of additional sites for hydration products, provided by the less reactive C_2S. This allows the nucleation of CSH to occur at sites remote from the C_3S, which is then free to hydrate further. It is postulated that the similar atomic composition and hydration products of the two phases makes the C_2S surface favorable as a site for the nucleation

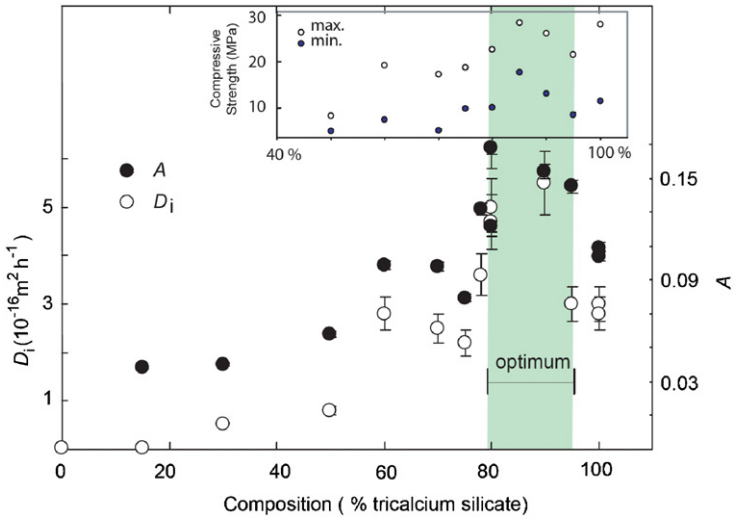

Fig. 4. Predicted amount of product A and diffusion coefficient D_i with mixture composition. Errors are one standard deviation, and in composition are smaller than the points. Inset shows the compressive strengths for mortars of the same components, comprising of 40–100% C_3S, after 28 d hydration.

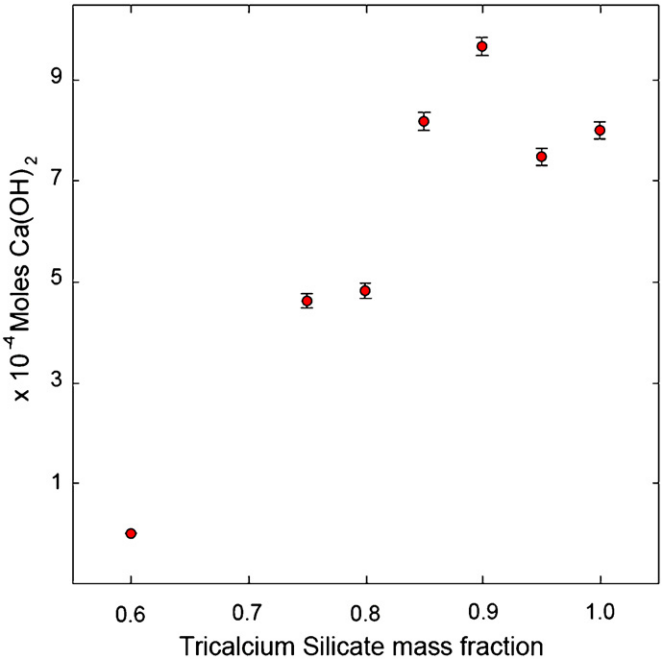

Fig. 5. Amount of $Ca(OH)_2$ produced at 22 h by various C_3S and C_2S mixtures, determined by INS. Errors, derived from mass error and fitting in DAVE, are one standard deviation, and in composition are smaller than the points.

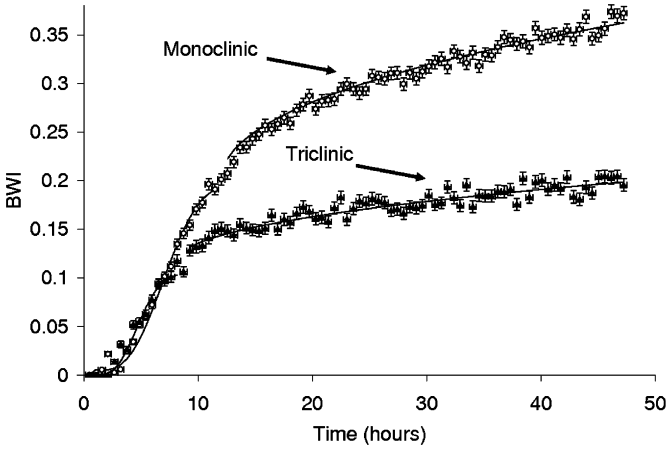

Fig. 6. Fits of hydration model s (solid likes) to the QENS BWI data (points) for triclinic and monoclinic C_3S pastes. Error bars represent absolute error.

and growth of products for the hydrating C_3S. It is advantageous to provide these nucleation sites using C_2S rather than inert particles because C_2S not only provides a favorable template, but eventually hydrates itself. Therefore C_2S enhances the later strength of the paste whereas inert particles do not.

3.2. Effect of crystal form on hydration

C_3S exhibits polymorphism, and in cement, it exists as a solid solution of ion stabilized forms. QENS results reveal that monoclinic and triclinic C_3S forms have very different hydration mechanics (Fig. 6). In particular, the rate of product formation during the nucleation and growth regime was found to be higher for monoclinic than for triclinic form. This in turn affects the total amount of product, and therefore differences in the strength in the early stage of hydration may arise. These results are listed in Table 2.

The INS results support these QENS results. Despite having almost half the surface area and marginally less C_3S than the triclinic sample, the monoclinic sample produces almost three times the amount of $Ca(OH)_2$. Hence, these results agree with the QENS results, which ultimately predicted that more products would be made by the monoclinic sample.

It is speculated that both the crystal form and the type of stabilizing ion entering the lattice affect the type of

Table 2
Hydration parameters for the induction and nucleation and growth period for triclinic (*T*), monoclinic (M), and mixtures (Mix) of C_3S.

	Radius (m)	Induction	Nucleation and growth (NG)		
		t_i (*h*)	d(BWI)/dt (h^{-1})	*A*	NG length (*h*)
T	4.9×10^{-6}	1.30 (8)	0.0184 (1)	0.104 (2)	6.9 (1)
M	1.7×10^{-5}	1.56 (8)	0.0201 (1)	0.193 (5)	10.5 (1)
Mix	4.9×10^{-6}	1.02 (8)	0.0159 (1)	0.129 (3)	9.9 (1)
Mix	1.7×10^{-5}	1.02 (8)	0.0159 (1)	0.129 (3)	9.9 (1)

Errors are absolute.

products that form during the nucleation and growth regime.

4. Conclusions

QENS and INS have been demonstrated as complimentary tools for the study of the complex hydration of the important and poorly understood calcium silicate phases in cement.

This study has shown that the overall hydration reaction of cement is more complex than a simple linear combination of the reactions for the individual components. Thus the hydration reactions do not occur independently in mixtures of C_3S and C_2S, the two crucial components of cement. Unexpectedly, favorable reaction mechanics occur when a mass fraction of 80–95% C_3S mixture is used, where it was previously thought that C_2S played no role during early hydration. Industrial cement clinker contains a mass fraction of approximately 70–80% C_3S out of the total calcium silicate phases, less than the amount determined from this work of 80–95% for optimal hydration mechanics, and strength, at 85%. This suggests that increasing the C_3S content by 5–15% may lead to improved cement. However, there are many other components in cement clinker and other interactions could also affect the performance of the final material.

INS and QENS also reveal a significant effect of crystal form and stabilizing ion on the hydration, indicating that more products would be made by monoclinic C_3S than by the triclinic form. Further work is needed to clarify if this increase translates to an increase in early strength of the paste, and to further explore the effect of stabilizing ions on the hydration.

Finally, the effect of additives on the hydration mechanics and product microstructure is in many cases largely unknown. Traditional methods such as calorimetry lack the sensitivity of the neutron methods presented here that allow the effects of these admixtures to be studied in more detail. QENS has already been applied to observe the effects of an effective retarder (sucrose), and effective accelerator ($CaCl_2$), to C_3S hydration mechanics [20,21].

Acknowledgements

We thank Craig Brown and Juscelino Leão from the NIST Center for Neutron Research. We acknowledge the support of the National Institute of Standards and Technology, U.S. Department of Commerce, in providing the neutron research facilities used in this work.

References

[1] H.F.W. Taylor, Cement Chemistry, Thomas Telford, London, 1997.
[2] V.K. Peterson, D.A. Neumann, R.A. Livingston, Mater. Res. Soc. Symp. Proc. 840 (2005) Q2.2.
[3] V.K. Peterson, D.A. Neumann, R.A. Livingston, J. Phys. Chem. B. 109 (2005) 14449.
[4] V.K. Peterson, D.A. Neumann, R.A. Livingston, J. Mater. Res. 21 (2006) 1836.
[5] V.K. Peterson, C.M. Brown, R.A. Livingston, Chem. Phys. 326 (2006) 381.
[6] V.K. Peterson, D.A. Neumann, R.A. Livingston, Chem Phys. Lett. 419 (2006) 16.
[7] A.J. Allen, J.C. McLaughlin, D.A. Neumann, R.A. Livingston, J. Mater. Res. 19 (2004) 3242.
[8] A. Faraone, E. Fratini, P. Baglioni, S.-H. Chen, J. Chem. Phys. 121 (2004) 3212.
[9] E. Fratini, S.-H. Chen, P. Baglioni, M.-C. Bellissent-Funel, J. Phys. Chem. B. 106 (2002) 158.
[10] S.A. FitzGerald, J.J. Thomas, D.A. Neumann, R.A. Livingston, Cem. Concr. Res. 32 (2002) 409.
[11] J.J. Thomas, S.A. FitzGerald, D.A. Neumann, R.A. Livingston, J. Am. Ceram. Soc. 84 (2001) 1811.
[12] S.A. FitzGerald, D.A. Neumann, J.J. Rush, D.P. Bentz, R.A. Livingston, Chem. Mater. 10 (1998) 397.
[13] J.J. Thomas, J.J. Chen, H.M. Jennings, D.A. Neumann, Chem. Mater. 15 (2003) 3813.
[14] R. Berliner, M. Popovoci, K.W. Herwig, M. Berliner, H.M. Jennings, J.J. Thomas, Cem. Concr. Res. 28 (1998) 231.
[15] S.A. Fitzgerald, D.A. Neumann, J.J. Rush, R.J. Kirkpatrick, X. Cong, R.A. Livingston, J. Mater. Res. 14 (1998) 1160.
[16] J.R. Copley, T.J. Udovic, J. Res. Nat. Inst. Stand. Technol. 98 (1993) 71.
[17] DAVE, National Institute of Standards and Technology Center for Neutron Research.
[18] J.J. Thomas, H.M. Jennings, Chem. Mater. 11 (1999) 1907.
[19] T.J. Udovic, D.A. Neumann, J. Leão, C.M. Brown, Nucl. Instr. and Meth. A. 517 (2004) 189.
[20] V.K. Peterson, M. Garci-Juenger, Physica B, in press.
[21] V.K. Peterson, M.C.G. Juenger, Chem. Mater., 2006, in preparation.